





Lipidomics and Redox Lipidomics Indicate Early Stage Alcohol-Induced Liver Damage

Jeremy P. Koelmel,^{1,2*} Wan Y. Tan,^{1,3*} Yang Li,² John A. Bowden,^{4,5} Atiye Ahmadireskety,⁴ Andrew C. Patt,⁶ David J. Orlicky,⁷ Ewy Mathé,⁶ Nicholas M. Kroeger,⁸ David C. Thompson,⁹ Jason A. Cochran,^{2,8} Jaya Prakash Golla ,¹ Aikaterini Kandyliari ,^{1,10} Ying Chen,¹ Georgia Charkoftaki,¹ Joy D. Guingab-Cagmat,² Hiroshi Tsugawa ,¹¹⁻¹³ Anmol Arora ,^{1,14} Kirill Veselkov,¹⁵ Shunji Kato,¹⁶ Yurika Otoki,¹⁶ Kiyotaka Nakagawa,¹⁶ Richard A. Yost,^{2,4} Timothy J. Garrett,^{2,4} and Vasilis Vasilou¹

Alcoholic fatty liver disease (AFLD) is characterized by lipid accumulation and inflammation and can progress to cirrhosis and cancer in the liver. AFLD diagnosis currently relies on histological analysis of liver biopsies. Early detection permits interventions that would prevent progression to cirrhosis or later stages of the disease. Herein, we have conducted the first comprehensive time-course study of lipids using novel state-of-the-art lipidomics methods in plasma and liver in the early stages of a mouse model of AFLD, i.e., Lieber-DeCarli diet model. In ethanol-treated mice, changes in liver tissue included up-regulation of triglycerides (TGs) and oxidized TGs and down-regulation of phosphatidylcholine, lysophosphatidylcholine, and 20-22-carbon-containing lipid-mediator precursors. An increase in oxidized TGs preceded histological signs of early AFLD, i.e., steatosis, with these changes observed in both the liver and plasma. The major lipid classes dysregulated by ethanol play important roles in hepatic inflammation, steatosis, and oxidative damage. **Conclusion:** Alcohol consumption alters the liver lipidome before overt histological markers of early AFLD. This introduces the exciting possibility that specific lipids may serve as earlier biomarkers of AFLD than those currently being used. (*Hepatology Communications* 2021;0:1-13).

Fatty liver disease or hepatosteatosis occurs when lipids accumulate in the liver as a result of dysregulated lipid metabolism leading to increased lipogenesis, reduced lipolysis, and lipotoxicity.⁽¹⁾ Lipotoxicity may potentially elicit an inflammatory response that can lead to the progression to cirrhosis and hepatocellular carcinoma. Clinically, fatty

liver disease can be divided into alcoholic (AFLD) and nonalcoholic fatty liver disease (NAFLD). Both AFLD and NAFLD are generally indistinguishable using only morphological evidence, other than the distinctions applied by these etiological designations.⁽²⁾ Although the prevalence of NAFLD worldwide compared to AFLD has been increasing exponentially

Abbreviations: AFLD, alcoholic fatty liver disease; ALD, alcoholic liver disease; ANOVA, analysis of variance; Cer, ceramide; DG, diglyceride; FDR, false discovery rate; LD, Lieber-DeCarli; LPC, lysophosphatidylcholine; LPE, lysophosphatidylethanolamine; NAFLD, nonalcoholic fatty liver disease; Ox, oxidized; PC, phosphatidylcholine; PCA, principal component analysis; PE, phosphatidylethanolamine; PG, phosphatidylglycerol; ROS, reactive oxygen species; SM, sphingomyelin; TG, triglyceride; vol, volume.

Received May 27, 2021; accepted August 4, 2021.

Additional Supporting Information may be found at onlinelibrary.wiley.com/doi/10.1002/hep4.1825/supinfo.

*These authors contributed equally to this work.

Supported by the National Institutes of Health, National Institute on Alcohol Abuse and Alcoholism (#R21AA028432, #R24AA022057 to V.V.).

© 2021 The Authors. *Hepatology Communications* published by Wiley Periodicals, Inc., on behalf of the American Association for the Study of Liver Diseases. This is an open access article under the terms of the Creative Commons Attribution-NonCommercial-NoDerivs License, which permits use and distribution in any medium, provided the original work is properly cited, the use is non-commercial and no modifications or adaptations are made.

View this article online at wileyonlinelibrary.com.

DOI 10.1002/hep4.1825

Potential conflict of interest: Dr. Thompson owns stock in Medtronic. Dr. Vasilis and Dr. Chen received grants from the National Institutes of Health. The other authors have nothing to report.

during the past decade due to the global obesity pandemic, attention to AFLD has been growing in recent years for a multitude of reasons.

The World Health Organization Global Status Report on Alcohol and Health 2018 reported an alarming 3 million deaths (5.3% of all deaths) and 132.6 million disability-adjusted life years (DALYs) from harmful alcohol use in the year 2016⁽³⁾; among them, alcohol-attributable liver cirrhosis caused a significant 607,000 deaths and 22.2 million DALYs.⁽³⁾ It has also become a more frequent cause of morbidity and mortality globally, especially in developing countries.⁽⁴⁾ Importantly, approximately half of liver cirrhosis-related deaths were attributable to alcohol use.⁽³⁾ The global burden of alcohol-related liver disease is postulated to increase with increasing alcohol consumption. A large comprehensive survey conducted in the United States since 2001 showed that alcohol use from 2001 to 2012 rose across all categories of alcohol use and all demographics. This rise was more pronounced in women, rural citizens, and those with lower socioeconomic status.⁽⁵⁾

Due to the high morbidity and mortality of advanced liver disease, detection of early stages of alcoholic liver disease (ALD) and development of new therapeutic agents are crucial. Currently, early forms of ALD are

often missed and mostly detected during the stage of alcoholic hepatitis when they are clinically apparent.⁽⁶⁾ Other than invasive liver biopsy, which has been the gold standard for diagnosis, no noninvasive techniques have been approved to diagnose the different stages of ALD.⁽⁷⁾ Once diagnosed, treatment options are limited. Standard therapy for the past decades has not evolved.⁽⁶⁾ In both early and severe ALD, prolonged abstinence is the most efficient therapeutic measure. Depending on the stages of ALD, steroids are used for alcoholic hepatitis and liver transplantation is needed at the end-stage disease.^(6,8) This is further hampered by poor understanding of the pathophysiology of ALD.

Recent advances in the field of lipidomics has allowed for the global characterization of lipids at the molecular and systems level. This advancement has permitted the identification of toxic lipid species and the unique molecular signatures for specific liver disease.⁽¹⁾ Lipidomics analysis has been shown to discern stages of NAFLD.⁽¹⁾ However, no work to date has employed the state-of-the-art lipidomics techniques to determine changes in lipid profiles across time in the early stages of AFLD. In our study, we were interested in assessing the dynamic changes in lipid profile of early stages of AFLD across time to determine early stage indicators and mechanisms of fatty liver disease

ARTICLE INFORMATION:

From the ¹Department of Environmental Health Sciences, Yale School of Public Health, New Haven, CT, USA; ²Department of Pathology, Immunology and Laboratory Medicine, University of Florida, Gainesville, FL, USA; ³Internal Medicine Residency Program, Department of Internal Medicine, Norwalk Hospital, Norwalk, CT, USA; ⁴Department of Chemistry, University of Florida, Gainesville, FL, USA; ⁵Center for Environmental and Human Toxicology and Department of Physiological Sciences, University of Florida, Gainesville, FL, USA; ⁶Division of Preclinical Innovation, National Center for Advancing Translational Sciences, National Institutes of Health, Rockville, MD, USA; ⁷Department of Pathology, University of Colorado School of Medicine, Denver, CO, USA; ⁸Computer and Information Science and Engineering, University of Florida, Gainesville, FL, USA; ⁹Department of Clinical Pharmacy, University of Colorado Skaggs School of Pharmacy and Pharmaceutical Sciences, University of Colorado, Aurora, CO, USA; ¹⁰Unit of Human Nutrition, Department of Food Science and Human Nutrition, Agricultural University of Athens, Athens, Greece; ¹¹RIKEN Center for Sustainable Resource Science, Kanagawa, Japan; ¹²RIKEN Center for Integrative Medical Sciences, Kanagawa, Japan; ¹³Department of Biotechnology and Life Science, Tokyo University of Agriculture and Technology, Tokyo, Japan; ¹⁴School of Clinical Medicine, University of Cambridge, Cambridge, United Kingdom; ¹⁵Department of Metabolism, Digestion and Reproduction, Imperial College, London, United Kingdom; ¹⁶Food and Biodynamic Chemistry Laboratory, Graduate School of Agricultural Science, Tohoku University, Sendai, Japan.

ADDRESS CORRESPONDENCE AND REPRINT REQUESTS TO:

Vasilis Vasilou, Ph.D.
Department of Environmental Health Sciences
Yale School of Public Health
60 College Street
New Haven, CT 06510
E-mail: vasilis.vasilou@yale.edu
Tel.: +1-203-785-2867

or
Timothy J. Garrett, Ph.D.
Department of Pathology, Immunology and Laboratory Medicine
University of Florida
Gainesville, FL 32611, USA
E-mail: tgarrett@ufl.edu
Tel.: +1-352-392-3261

progression. This technique is promising not only for the development of biomarkers for detection of early stages of AFLD and insights into the pathophysiology of AFLD but also for novel therapeutic intervention.

Materials and Methods

MICE STUDY

Twelve-week-old male C57BL/6J mice were fed a modified Lieber-DeCarli (LD) liquid diet containing ethanol (ethanol group E1-3, $n = 7-10$) or the control LD diet in which ethanol was substituted isocalorically by maltose-dextrin (control group C1-3, $n = 5-7$) for 5 weeks. The levels of ethanol in the AFLD diet started at 2% (volume [vol]/vol) and was increased by 1% weekly over the following 5 weeks (Fig. 1). The increased amount of ethanol replaced maltose isocalorically in the diet; therefore, the calories per unit volume liquid diet stayed the same throughout the feeding course. The control groups were pair fed such that they received the same amount of food (or calories) consumed by the ethanol groups.

Calorie intake (kilocalories) was recorded (Supporting Table S2; Supporting Fig. S9), and after adjusting the P value using the Benjamini-Hochberg correction, no differences between ethanol-fed and control mice were observed (false discovery rate [FDR] corrected $P < 0.05$); however, calorie intake in weeks 3-5 was slightly higher in control-fed mice and approaching significance. Livers were harvested on weeks 0 (chow), 2 (GE1, GC1), 4 (GE2, GC2), and 5 (GE3, GC3) (Fig. 1), and untargeted lipidomics was performed.

HISTOPATHOLOGY

A section of the liver from each mouse was processed for hematoxylin and eosin staining using standard procedures and examined by an experienced pathologist blinded to the study. Score averages, SDs, and P values were determined using the two-sided, unpaired, or unequal variance Student t test.

LIPIDOMICS

Liver and plasma samples were extracted using the Bligh-Dyer extraction method.⁽⁹⁾ Liquid chromatography

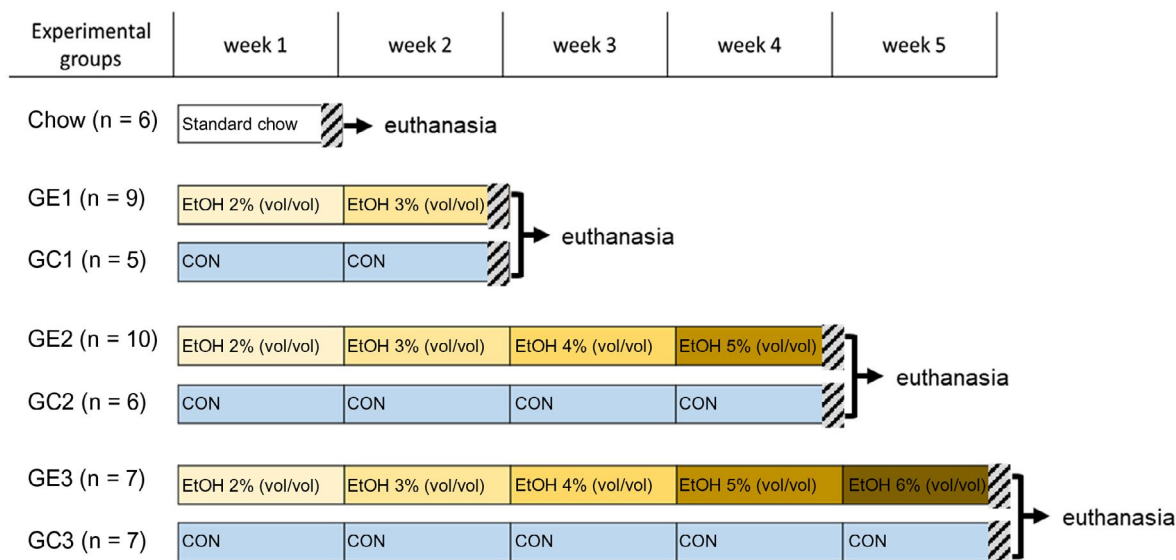


FIG. 1. Scheme of treatment regime. Male C57BL/6J mice (10-12 weeks old) were randomly divided into seven groups. The chow group was fed standard rodent chow. EtOH groups (GE1, GE2, GE3) and pair-fed control groups (GC1, GC2, GC3) were fed a modified LD diet for up to 5 weeks. GE groups started with an LD diet containing 2% EtOH vol/vol with a weekly increase of 1% EtOH (vol/vol) until it reached 5% (vol/vol). GC groups received an LD diet (CON) in which the EtOH content was substituted by carbohydrates. On day 6-7 (3 PM to 9 AM) of week 2 (GE1 and GC1), week 4 (GE2 and GC2), or week 5 (GE3 and GC3), mice were placed singly in a metabolic cage with free access to the corresponding LD diet for 18 hours and then subjected to 4 hours fasting in regular housing cages before being euthanized. Abbreviations: CON, control; EtOH, ethanol.

was performed on an ultra-high-performance liquid chromatography (UHPLC) system (Vanquish; Thermo Scientific, San Jose, CA) using a C₃₀ column (2.1 × 150 mm, 2.6 μm particle size) (Accucore; Thermo Scientific) and a gradient program consisting of mobile phase A (60:40 acetonitrile/water) and mobile phase B (90:10 isopropanol/acetonitrile), each containing 5 mmol/L ammonium formate and 0.1% (vol/vol) formic acid. The UHPLC system was coupled to a mass spectrometer (Q-Exactive Orbitrap; Thermo Scientific) for chromatographic separation and mass spectral measurement of lipids in positive and negative ion mode, respectively, using full-scan and iterative exclusion^(10,11) tandem mass spectrometry. The software LipidMatch Flow⁽¹²⁾ was deployed for peak picking, blank filtering, annotation, and combining positive and negative ion polarity, whereas LipidMatch Normalizer⁽¹³⁾ was used for semiquantitation. Novel oxidized lipidomics libraries were developed and applied as reported.⁽¹⁴⁾ Extensive details on software development, deployment, and acquisition methods can be found in the Supporting Material.

Results

Although current state-of-the-art lipidomics technology can only provide estimated lipid concentrations using class-based standards, as has been done here, these relative concentrations are sufficient for determining lipid fold changes.⁽¹⁵⁾ Further discussion on lipid normalization is discussed in depth elsewhere.^(13,16) Significant changes across nearly all lipid classes were observed for alcohol-fed mice both across time and in relation to the controls (Fig. 2).

TIME- AND DOSE-DEPENDENT CHANGES IN ALCOHOLIC LIVER LIPIDOME ACROSS 13 LIPID CLASSES

A diverse group of liver lipids significantly changed in concentration across time and dose in alcohol-fed mice. Of the 960 lipid species annotated in the liver, 297 lipid species across 13 lipid classes had statistically significant differences between controls and alcohol-fed mice at 4 and 5 weeks as well as significant differences between weeks 2 and 5 of the alcohol-fed diet (using FDR [Benjamini-Hochberg]-corrected analysis of variance

[ANOVA] with Tukey *post hoc* analysis). A large percentage (25% or greater) of species within a class of those lipid classes shown in Fig. 2 (and Supporting Table S1A) all changed in the same manner with continued consumption of alcohol (Fig. 2 is derived from Supporting Table S1A,B). For certain lipid species, changes occurred in the same direction within a lipid class.

The advantage of mass spectrometry-based lipidomics is the identification of fatty acyl constituents in intact lipids. As this technique has only gained popularity within the last decade, minimal information is available about individual intact lipid species and their biology. Certain lipid classes contained both increasing and decreasing lipid species in samples from ethanol-fed mice (Fig. 2), including phosphatidylethanolamines (PEs) (Supporting Fig. S3A), diglycerides (DGs) (Supporting Fig. S3I), sphingomyelins (SMs) (Supporting Fig. S3O-P), ceramides (Cers) (Supporting Fig. S3Q), and phosphatidylglycerols (PGs). Selected individual lipids with significant changes across time and between alcohol-fed and pair-fed control mice are shown in Supporting Fig. S3A-S.

Over 10% of long and short chain oxidized triglycerides (OxTGs) increased across all time points, and over 85% (Supporting Table S1A) were significantly higher than controls for weeks 4 and 5. In addition, OxTGs were the only lipid class with over 10% of species higher in alcohol-fed mouse than controls for the first time point (week 2; Fig. 2). LipidMatch Flow libraries contain both short chain (aldehyde and carboxylic acid terminus) and long chain (hydroperoxyl, hydroxyl, ketone, and epoxy) oxidized species. OxTGs were found to increase with ethanol feeding irrespective of the type of oxidation product (Supporting Fig. S3J-L). TGs were not the only lipids species to be oxidized following exposure to ethanol; certain oxidized glycerophospholipids, for example, OxPGs(18:1_18:1[OH]) and oxidized phosphatidylcholines (OxPCs)(16:0_18:2[OH]) were also observed to increase (Supporting Fig. S3M).

A total of 66% of TGs increased between weeks 2 and 4, and no TGs changed significantly between weeks 4 and 5 of ethanol feeding. A large proportion of the TGs in the ethanol-fed group were significantly higher compared to the control group after week 2 (85% of TGs were higher during week 4 and 33% were higher during week 5 in the ethanol-fed group compared to the control group).

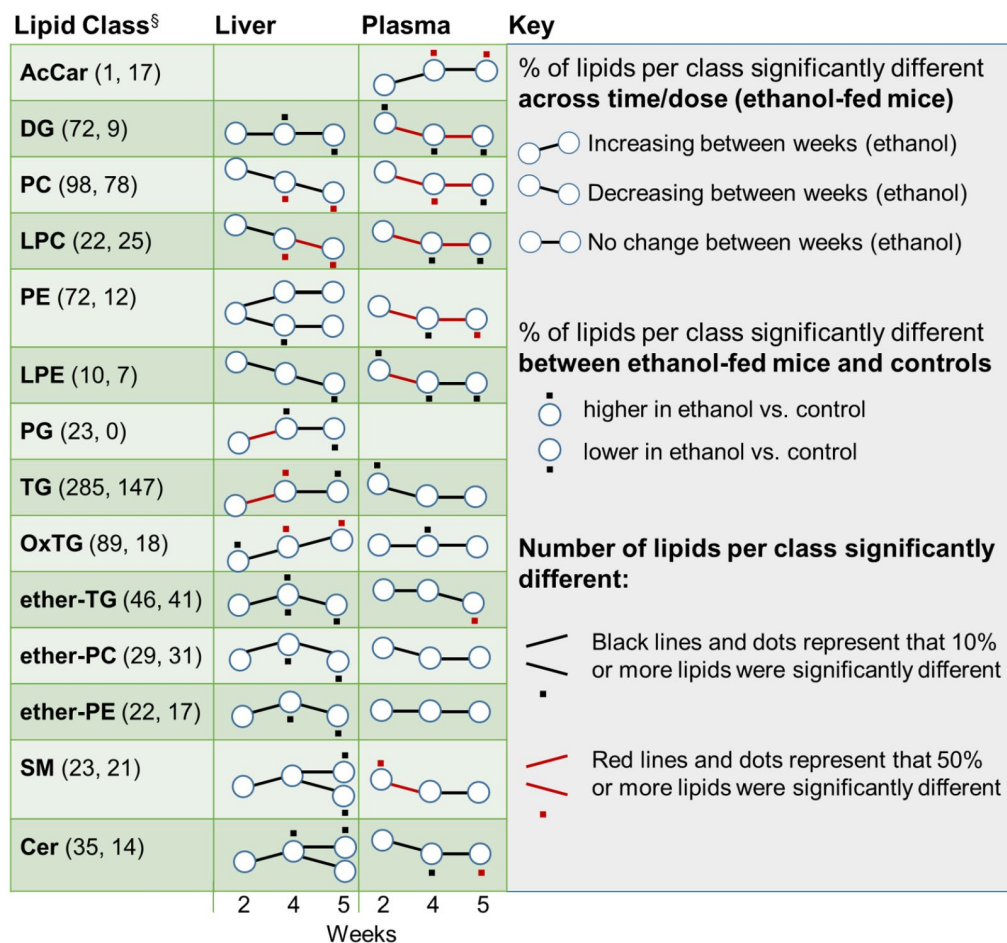


FIG. 2. Percentage of liver and plasma lipids per class significantly up-regulated or down-regulated across time and in comparison to controls. Alterations (increases or decreases) in classes of lipids in ethanol-consuming mice are expressed as a categorical percentage change relative to levels (i) at previous treatment times (2, 4, or 5 weeks) or (ii) in control mice at the same treatment time. Line direction(s) represent the direction of differences between treatment times, whereas the position of colored squares (above or below the circle) indicates whether lipids are higher in ethanol-fed mice or controls. Significantly up-regulated and/or down-regulated lipid species were determined by an FDR-corrected ANOVA with Tukey *post hoc* test, with $P < 0.05$ and a fold change of 1.25 (or 0.8 if lipid levels in ethanol-fed mice were lower than controls or previous time points). [§]Values in parentheses represent the number of species per class annotated by LipidMatch Flow for liver and plasma samples, respectively. Abbreviation: AcCar: acylcarnitine.

We found that 37% of PCs from the liver tissue had decreased between weeks 2 and 4 and 43% had decreased between weeks 4 and 5 in the ethanol group. Compared to the control group, the ethanol-fed group had 52% of PCs lower during week 4 and 61% of PCs lower during week 5.

In the ethanol group, 41% of lysophosphatidylcholines (LPCs) from the liver tissue decreased between weeks 2 and 4 and 64% decreased between weeks 4 and 5. Compared to the control group, the ethanol-fed group had 64% of PCs lower during week 4 and 77% of PCs lower during week 5.

Also in the ethanol group, 20% of lysophosphatidylethanolamines (LPEs) from the liver tissue decreased between weeks 2 and 4 and between weeks 4 and 5. Compared to the control group, 30% of LPEs in the ethanol-fed group were lower during week 4 and 40% of LPEs were lower during week 5.

Over 10% of ether lipids (50% ether-TG, 10% ether-PC, and 32% ether-PE) from the liver tissue significantly increased from week 2 to week 4 in both alcohol-fed and control mice, followed by a significant decrease from week 4 to week 5 of alcohol-fed mice (37% ether-TG, 10% ether-PC, and 14% ether-PE).

The ethanol-fed group had lower ether lipids by the end of week 5 compared to the control group (48% ether-TGs, 41% ether-PCs, and 32% ether-PEs were lower in ethanol-fed mice).

By the end of week 5 of ethanol feeding, all Cers and SMs contained 20-22 carbons in their fatty acyl chain, i.e., a 24:1 decrease in alcohol-fed mice.

No major percentage increase or decrease in diacylglycerols was observed across time and dose in the ethanol group. However, at week 2, 32% of DGs were higher in the ethanol group compared to the control group, whereas at week 5, 9% of DGs were higher in the ethanol group and 19% of DGs were higher in the control group.

There was an increase of 18% of PEs and a decrease of 22% of PEs in the ethanol-fed group at week 2. In addition, 61% of PGs increased at week 2 in the ethanol-fed group, and 30% of PGs were higher than the control group at week 2. At week 5, 13% of PGs were higher in the control group compared to the ethanol-fed group.

LIPID CHANGES IN PLASMA AND CORRELATIONS TO LIVER LIPIDS

While mice generally were separated in principal component analysis (PCA) using liver lipid profiles according to ethanol treatment versus controls, minimal separation was obtained in plasma (Supporting Fig. S2). No PCA scores were significant between groups for mouse plasma except between GE1 and GE2. For mouse liver, the following were significant (FDR corrected $P < 0.05$ using Benjamini-Hochberg): chow versus GE1, GC2 versus GE2, GC3 versus GE3, GE1 versus GE3, and GE1 versus GE2 (Supporting Fig. S2). Observed changes in plasma did not generally correspond to lipid changes in liver, although certain lipid species followed similar trends (Fig. 3A-D). One OxTG in the plasma, OxTG(18:2_18:2_18:2 [ketone]), was significantly higher at all time points in ethanol-fed versus control mice (Fig. 3B). This species was over an order of magnitude higher in the liver at both weeks 4 and 5 than in the plasma and showed similar trends compared to plasma (Fig. 3A).

Pearson's correlation across 336 lipids annotated in both plasma and liver showed that about 18% of lipids correlated with a Pearson's value of 0.4 or higher and a significant FDR-corrected P value (Benjamini-Hochberg corrected), whereas only seven correlated

with a Pearson's correlation greater than 0.7. Of the lipids with Pearson's correlation above 0.4, 84% consisted of lipids containing at least one fatty acid between 20 and 22 carbons in length. Also, lipids correlating between plasma and liver mainly consisted of sphingolipids (only those with 20:0 or 22:0), PCs, and LPCs. The PCs and LPCs were significantly down-regulated in the ethanol-fed mice at 4 and 5 weeks. For example, LPC(20:0), which had one of the strongest correlations between plasma and liver (Supporting Fig. S8; Pearson's value, 0.73), was also found to be 17-fold higher in week-2 ethanol-fed mice compared to the ethanol-fed mice at weeks 4 and 5. This LPC was also 16-fold higher in respective controls compared to ethanol-fed mice at weeks 4 and 5. Because the plasma levels of these lipids reflect changes in the liver, these lipids serve as biomarker candidates for ethanol damage to the liver.

Plasma lipid changes in response to alcohol feeding appeared to depend on the dose and/or duration of alcohol feeding. For example, nearly all lipid classes with significant changes in alcohol-fed mice (DG, PC, LPC, PE, LPE, TG, ether-TG, SM, and Cer) were found to be reduced during weeks 4 and 5. By contrast, a few (DG, LPE, TG, and SM) were elevated in week 2 relative to pair-fed controls (Fig. 2). One exception to the decrease in lipid classes by week 4 was acylcarnitine; over 50% of the 17 annotated species were elevated in alcohol-fed mice in both weeks 4 and 5 of feeding (relative to pair-fed control mice) (Fig. 1; Supporting Fig. S4C).

The plasma levels of most glycerophospholipids (>50%) were reduced by week 4 (Supporting Fig. S5D). Of the decreased glycerophospholipids, a large proportion contained 20:4 (Fig. 4D), and five of the top six most significantly changed species contained 20:4 (Supporting Fig. S4D). The fatty acyl trends observed in liver were reproduced in plasma, with down-regulated sphingolipids containing only 20-22 carbons (except for 24:1) in both liver and plasma (Fig. 4A,C). A boxplot for one of the most significantly altered sphingolipids in plasma, HexCer(d18:1/22:0) (Fig. 3D), is shown alongside the corresponding lipid boxplot in liver (Fig. 3C). Glycerophospholipids also showed trends in the frequency of fatty acyl chains across down-regulated lipids, with these down-regulated lipids in both plasma and liver containing mainly 20-22 carbons in the longest fatty acyl chain, with 20:4, 22:6, and

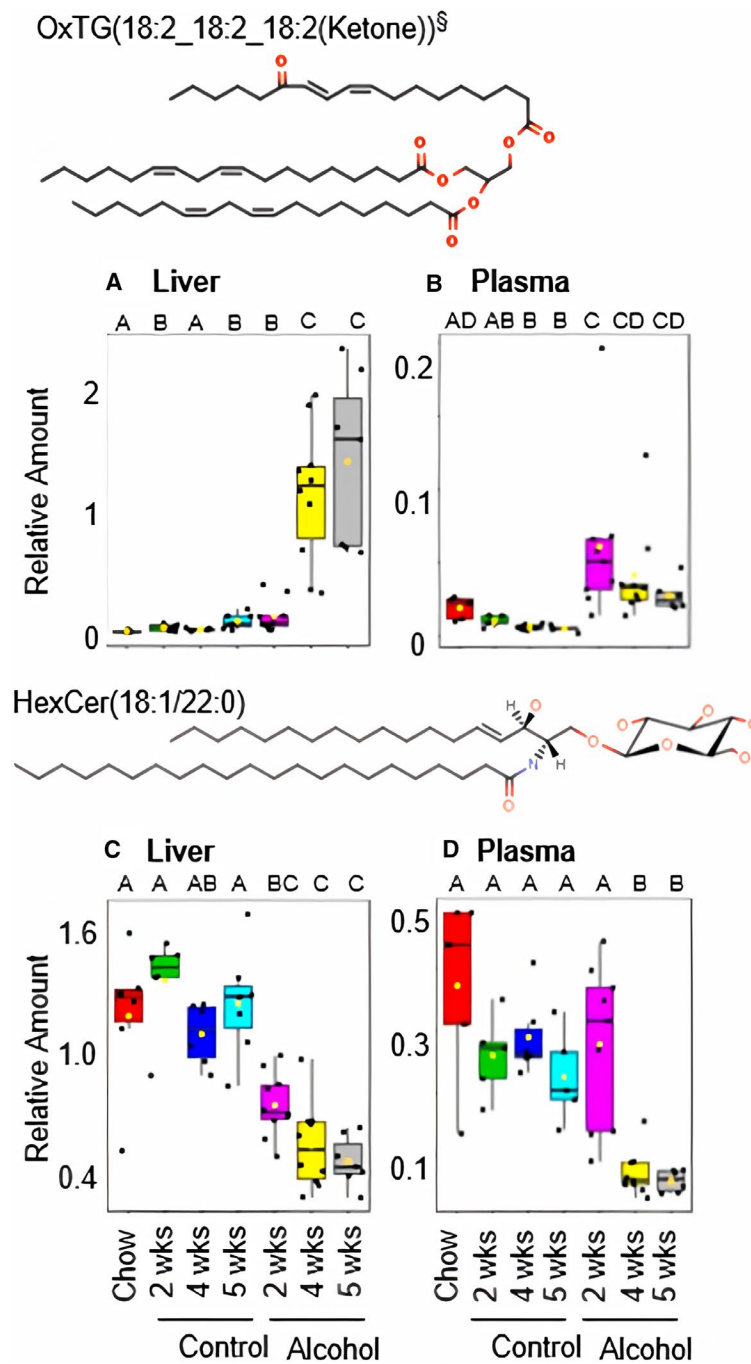


FIG. 3. Boxplots of an OxTG and HexCer lipid molecule with significant changes across time and between ethanol-fed and control mice. Minimum, first, second, and third quartile and maximum were used to generate boxplots; individual samples are also shown (dots). Relative amounts of OxTG(18:2_18:2_18:2[ketone]) in (A) liver and (B) plasma; (C) HexCer(d18:1/22:0) in liver and (D) plasma are shown (class-based internal standard normalization applied). Both species show significant changes across time points and between alcohol-fed and control (pair-fed) mice. Significance was determined by an FDR (Benjamini-Hochberg)-corrected ANOVA with Tukey *post-hoc* test ($P < 0.05$). Groupings with the same letters are not significantly different from one another, whereas those without the same letters are. [§]The peak representing OxTG(18:2_18:2_18:2[ketone]) also consisted of OxTG(16:0_18:2_20:4[ketone]) as a smaller fraction. Abbreviations: HexCer, hexosylceramide; wks, weeks.

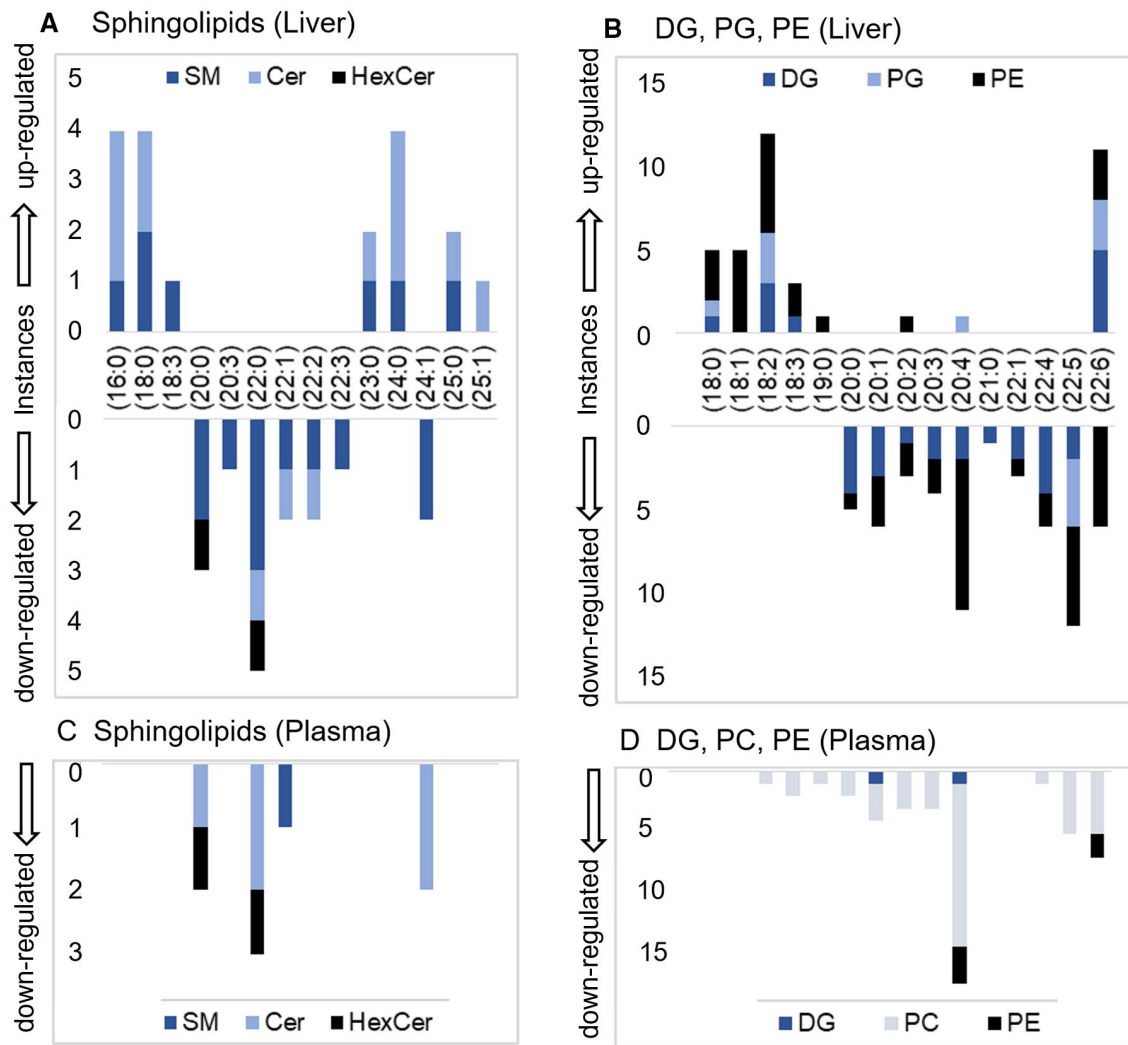


FIG. 4. Number of instances (frequency) of fatty acyl constituents in up-regulated and down-regulated lipids (y axis) in 5 weeks for alcohol-fed mice versus controls colored by lipid class. Fatty acyl constituents are shown across the x axis. Lipids contain one or more fatty acyl constituent bound to a backbone and head group, and the up-regulation or down-regulation of lipids containing these fatty acids can be indicative of the release of these fatty acids for downstream signaling in certain pathways (e.g., inflammatory pathways). The instances (frequency) of fatty acyl constituents contained in lipids that were up-regulated (i.e., higher in alcohol-fed mice compared to pair-fed controls) or down-regulated (i.e., lower in alcohol-fed mice compared to pair-fed controls) are shown (A) for HexCer, Cer, and SM in liver; (B) for DG, PE, and PG in liver; (C) for HexCer, Cer, and SM in plasma; (D) for DG, PE, and PC in plasma samples. Significant changes ($P < 0.05$) between lipids in the alcohol fed-group and the control group were determined by an FDR-corrected (Benjamini-Hochberg) ANOVA followed by Tukey *post hoc* test. For sphingolipids shown in (A), the fatty acyl chain on the sn2 position was used to calculate frequencies, whereas for DG, PG, PC, and PE, the longest carbon chain (or both if carbon chain lengths were equal) was used for the fatty acyl frequency calculations. On the plot, 0 refers to no significant lipids contained the corresponding fatty acyl constituent. Abbreviation: HexCer, hexosylceramide.

22:5 most frequently occurring (Fig. 4B,D). In contrast, docosahexaenoic acid (22:6)-containing species were the only lipids with 20-22-carbon chains, with a large percentage of species up-regulated as well as down-regulated in ethanol-fed mice versus controls (Fig. 4).

DOWN-REGULATION OF 20-22 CARBONS AND 24:1 FATTY ACYL CHAINS IN ALCOHOL-FED MICE

Sphingolipids are important species for numerous biological functions, including signaling related to

apoptosis, cell differentiation and growth, and inflammation. All sphingolipids that decreased in alcohol-fed mice contained 20–22 carbons in their fatty acyl chain or 24:1 (Fig. 4A). By contrast, sphingolipids with shorter chains (16–18 carbons) or longer chains (23–25) increased significantly by week 4 (Figs. 2, 4A). For example, for sphingolipids, Cer(d18:3/24:0), Cer(d18:1/24:0), Cer(d18:2/24:0), and SM(d18:2/24:0) were all significantly up-regulated, and therefore there is a frequency of 4 under 24:0 (Fig. 4A). Similarly, DGs, PGs, and PEs, which were down-regulated in the alcohol-fed group by week 5, all had at least one fatty acyl chain with 20–22 carbons (Fig. 4B). With the exception of two of 26 up-regulated species and 22:6, no up-regulated DG, PE, or PG had 20–22 carbons (Fig. 4B). In addition to certain DGs, PEs, and PGs (Fig. 4B) containing 22:6, ether-PE(P-20:0/22:6) was the only ether lipid to increase in alcohol-fed mice (the majority decreased by week 5) (Supporting Fig. S3E).

HISTOLOGY AND CORRELATION TO LIPID PROFILES

Histology was performed on all tissue sections that had lipidomics performed. Evidence of cell injury, inflammation, reactive changes, and steatosis was documented (see Supporting Material and Supporting Fig. S1) using published methods.⁽¹⁷⁾ Of these, only the total score for steatosis was significantly higher in alcohol-fed mice, i.e., in weeks 4 and 5 of alcohol feeding (relative to pair-fed control mice; see Supporting Material and Supporting Fig. S1). Histologically, only steatosis was significantly higher in alcohol-fed mice at week 4 ($P = 0.001$; mean score \pm SD ethanol group, 0.65 ± 0.034 ; mean score controls, 0). TG levels followed the same trend with over 50% increases in weeks 4 and 5 of ethanol feeding (Fig. 2). Whereas the use of histology was unable to delineate signs of steatosis in a number of the week-4 and week-5 alcohol-fed mice, lipidomics revealed that for certain TGs, such as TG(17:0_18:2_22:6), the concentration in every alcohol-fed mouse was higher than in pair-fed controls (Supporting Fig. S3F). These results suggest that lipidomics may be a more sensitive approach than histology to characterize the development and degree of steatosis. In addition, whereas histology only indicated that one mouse had signs of steatosis in the week-5 control (pair-fed) liquid diet (which contains high-fat

content by design) mice, lipidomics revealed that for numerous TGs, there was a significant increase compared to week-2 and week-4 control mice. This reveals that lipidomics may also be more sensitive to signs of steatosis from a high-fat diet, i.e., identifies changes before histological detection is possible.

Discussion

Only limited studies have been conducted on chronic alcohol-induced effects on the hepatic lipodome (see review by Clugston et al.⁽¹⁸⁾). Our study is unique compared to previous studies in the use of LipidMatch Flow and a time-course experiment that provides unprecedented detail on the diversity of lipid changes across early stages of liver damage caused by alcohol consumption. We provide evidence of hepatic inflammation, steatosis, and oxidative damage at early stages of alcohol consumption based on lipid changes (Figs. 2 and 5) and show that lipidomics is more sensitive to pathophysiological changes than histology. We also propose mechanisms underlying these changes (below).

In the present study, a decrease in both hepatic and plasma PC and LPC levels were observed in ethanol-fed mice across the three feeding durations (Fig. 2). While mice generally were separated in PCA according to ethanol treatment using liver lipid profiles, minimal separation was obtained in plasma. This suggests that other factors beyond treatment with ethanol had a strong effect on the lipid profiles observed in plasma. This is expected because the direct target of ethanol is the liver whereas the plasma reflects a mixture of lipids from numerous organs.

An explanation for the observed decrease in PC is the shift toward synthesis of TGs through initial conversion of PCs to DGs. DGs fuel the synthesis of TGs during hepatic steatosis. This is supported by the up-regulation of DG acyltransferase 2 (DGAT2) reported for chronic alcohol consumption, an isoform predominantly expressed in the liver that plays a regulatory role in TG biosynthesis, fatty acid homeostasis, very low-density lipoprotein (VLDL) assembly, and positive regulation of hepatic stellate cells.^(19,20) Interestingly, while histological assessment of liver tissues found no significant difference between steatosis in ethanol-treated and control mice except in week 4 (Supporting Fig. S1; only approaching significance for

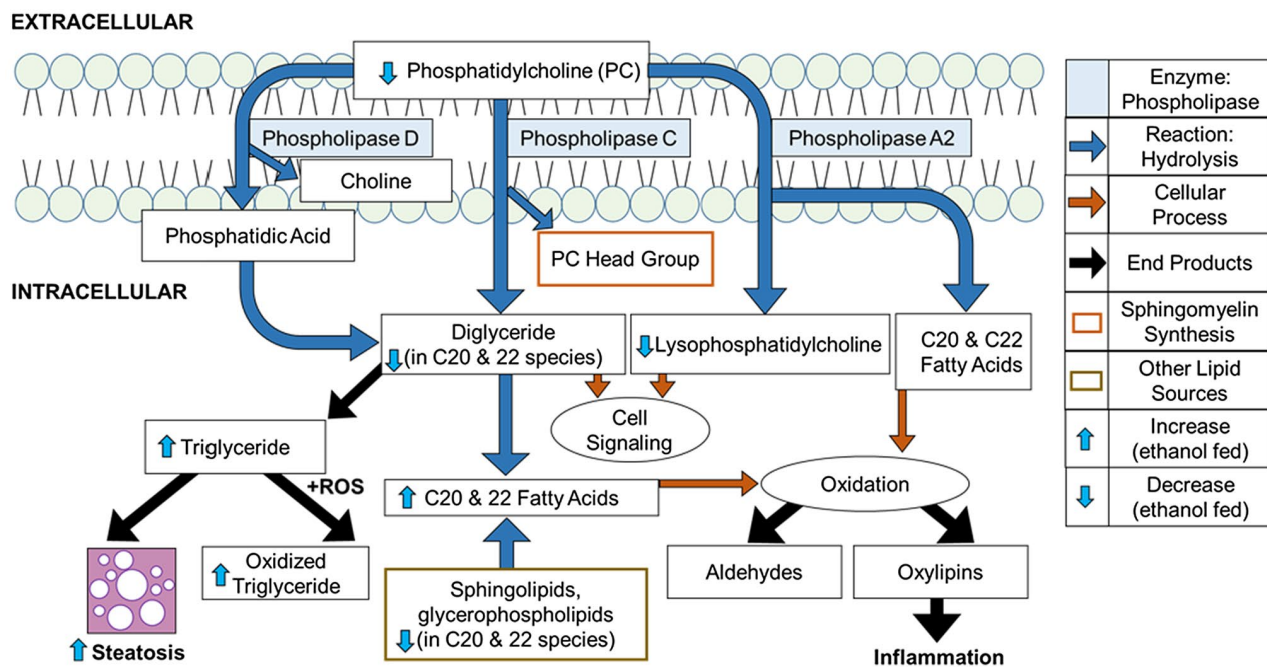


FIG. 5. Lipid changes in mouse liver determined by LipidMatch Flow indicative of steatosis, oxidative damage, and inflammation in ethanol-fed mice. PC is hydrolyzed by three phospholipase enzymes (D, C, and A₂) at the plasma membrane. Phospholipase D results in the synthesis of phosphatidic acid and choline; phospholipase C results in DG and phosphatidylcholine head group, which is used in SM synthesis; and phospholipase A₂ forms LPC and fatty acids. DG and LPC are involved in intracellular cellular signaling. DG can undergo acylation to form TG (leading to steatosis). TG undergoes further oxidation by ROS to form OxTG. C20 and C22 fatty acids are released from various sources, such as DGs, sphingolipids, and PEs. They can undergo oxidation, forming oxylipins and aldehydes. Oxylipins, such as eicosanoids, are then used in cellular signaling, such as in the inflammatory pathway. Aldehydes can cause cellular damage or undergo further reaction, such as carbonylation to form signaling molecules or dehydrogenation to form acetate.

week 5), significant differences were obtained in lipidomic results for TGs in both weeks 4 and 5, showing that use of a lipidomics approach may be a more sensitive and accurate tool to identify steatosis than histology (Fig. 2).

Sphingolipids play vital roles as regulators of many cellular processes, such as cell growth, apoptosis, cell senescence, inflammation, and intracellular trafficking, in response to cellular stress.⁽²¹⁾ We observed a differential decrease and increase in specific SM and Cer species, with those containing predominantly C20 and C22 fatty acyl chains decreasing after 4 weeks of ethanol feeding and certain species increasing between weeks 2 and 4 (Fig. 4A). Arachidonic acid (20:4) serves as a precursor for proinflammatory mediators.⁽²²⁾ As such, 20:4-containing glycerophospholipids may serve as a source of 20:4 for an inflammatory response, explaining the decrease. Ethanol has been shown to induce increased levels of hepatic Cers and increased sphingosine and sphinganine in

mice, with the latter two being precursors for Cer production.^(23,24) Sphinganine and sphingosine were also found to be increased significantly compared to controls in our study. Cer can also be generated from SM hydrolysis by acidic sphingomyelinase (Smpd1) activity, which is increased by alcohol,⁽²⁴⁾ although corresponding SMs were not up-regulated, suggesting the prior route of synthesis. It is, however, important to note that the regulation of Cer levels is complex and can occur in numerous distinct mechanisms depending on organelle location and other signaling cascades.⁽²¹⁾ Increased hepatic Cer has downstream implications for the induction of hepatic steatosis. Cer is a known activator of protein phosphatase 2 through acid sphingomyelinase activation. Increased protein phosphatase 2 activity inhibits 5' adenosine monophosphate-activated protein kinase phosphorylation, which leads to activation of sterol regulatory element-binding protein 1 and acetyl-coenzyme A carboxylase. This enhances lipogenesis and depresses

fatty acid oxidation, leading to the accumulation of TGs in the liver and induction of steatosis.^(23,25-27)

Interestingly, we observed a decreasing trend in C20- and C22-containing lipids, both in the sphingolipids (Fig. 4A), and from DGs, PEs, and PGs (Fig. 4B). The selective reduction in certain C20- and C22-containing lipids may be explained by the release of the respective fatty acids by lipases to induce an inflammatory response through oxylipin synthesis (Fig. 5).⁽²⁸⁾ The decrease in certain C20 and C22 fatty acyl-containing lipids suggests that these fatty acids are used as cellular messengers and signaling molecules in the inflammatory pathways before microscopic changes are observed related to inflammation (Supporting Fig. S1). These changes can be protective, for example, docosahexaenoic acid (22:6) can reduce the inflammatory response and insulin resistance,⁽²⁹⁾ and therefore the increase in some lipids containing 22:6 may be protective if released for resolving production.

While PE containing 20-22 carbons decreased, over 10% of species detected were increased by week 5 (Fig. 2); for PCs, over 50% of species were found to be significantly lower by week 5 than in controls, whereas no species increased. The concomitant changes in the levels of PC and PE have significant implications. The ratio of PC to PE influences membrane integrity and plays a role in the progression of steatosis to steatohepatitis. In one study, a decreased PC/PE ratio led to progression of steatosis to steatohepatitis, whereas an increased PC/PE ratio *in vivo* reversed steatohepatitis but not steatosis.⁽³⁰⁾ The decrease in PE may be attributed to oxylipin synthesis, as discussed before, and to increased conversion of PE to PC by the action of PE N-methyltransferase, which has higher preference for arachidonic acid-containing PEs (which were the most drastically reduced in our study) and is shown to increase after short-term alcohol treatment.⁽³¹⁾ The increased levels of PE species not containing C20 and C22 is postulated to be a form of compensatory reaction toward depleted PC (as discussed before) because PE is the second most abundant phospholipid of most cell membranes after PC.

Plasmalogens, being the most abundant ether lipid, play an important role as endogenous antioxidants due to the presence of a vinyl ether bond that is susceptible to oxidation and termination of the chain-propagating step of oxidative damage to lipid membranes and

droplets.^(32,33) We found that ether lipids (ether-PC, ether-PE, and ether-TG) were lower in alcohol-fed individuals compared to the control in all groups, with over 25% of species increased between weeks 2 and 4 in ethanol-fed mice. Ethanol metabolism results in synthesis of reactive oxygen species (ROS) that preferentially oxidize plasmalogen due to the reactive vinyl ether bond, consistent with the decrease in the alcohol-fed group compared to the control. However, we also observed an increase in over 25% of ether-linked lipids between weeks 2 and 4. This suggests that despite the decrease levels of ether lipids due to their role as a sacrificial antioxidant, we postulate that there is increased synthesis of ether lipid at the peroxisome–endoplasmic reticulum pathway as a protective response to cellular damage caused by ROS during ethanol metabolism. Studies have shown the protective role of plasmalogen against hepatic steatosis and steatohepatitis in nonalcoholic steatohepatitis (NASH).^(34,35) This supports our finding of steatosis in the setting of low ether lipid level due to oxidative stress damage. However, we did not find studies investigating the effects of ethanol on the expression of genes and enzymes in ether lipid metabolism. Interestingly, we also observed a significant decrease (over 20-fold) in docosahexaenoic acid (C22:6)-containing ether-TGs in the ethanol-fed group (Supporting Fig. S7). A decrease in 22:6-containing TGs has been shown in steatosis in NASH but not in those with simple hepatic steatosis.⁽³⁵⁾ Along with ether-TGs containing 22:6, a number of other lipids containing high levels of polyunsaturated fatty acids were found to have the lowest correlation coefficient versus oxidized lipids (Supporting Fig. S6). Under oxidative stress, polyunsaturated fatty acids are preferentially oxidized over monounsaturated fatty acyl-containing lipids to form peroxides and aldehydes, which are lipotoxic and can modify lipids, proteins, carbohydrate, and DNA. Importantly, polyunsaturated aldehydes can undergo protein carbonylation, which then plays a role in the redox cellular signaling mechanism, mitochondrial dysfunction, and endoplasmic reticulum stress in response to oxidative stress.⁽³⁶⁾ One of the most sensitive changes in lipids was for OxTGs, which are direct products of oxidative stress and were found to increase before any other lipid changes were observed at the class level (Fig. 2). This suggests that certain OxTGs may be sensitive biomarkers in liver and plasma of early stage alcohol-induced liver

damage (Figs. 2, 3, and 5). It is interesting to note that primary, secondary, and tertiary oxidation products were observed, suggesting that lipidomics can be used to determine different stages of oxidative damage in tissues.

An important future step would be to translate observations and mechanistic insights in animal studies to specific impacts of alcohol on the human liver and blood plasma lipidome. Humans undergo similar responses to alcohol consumption as observed in mouse models; increase hepatic lipogenesis is observed in both mouse and humans after alcohol consumption,^(37,38) and ethanol promotes the formation of lipid droplets in the liver and reduces the secretion of VLDL.⁽³⁹⁾ Human studies applying lipidomics to ALD are lacking, but current consensus on multiple model systems show an increase in 18-carbon fatty acid-containing lipids. Furthermore, lipidomics studies on nonalcoholic liver disease in humans show changes in lipids (including certain sphingolipids) involved in the inflammatory responses⁽⁴⁰⁾ and more direct changes related to cell damage, for example, the generation of oxidized lipid species.⁽⁴¹⁾ These results in humans align with the results from our mouse model where we also show fat droplet accumulation by histology (Supporting Fig. S1), increases in 18-carbon fatty acid-containing lipids (Fig. 4), changes in sphingolipids indicative of inflammation (Fig. 4), and a drastic and early rise in oxidized lipids (Fig. 2). Therefore, results in our current study both expand on and align with the limited findings in human subjects, and more human-based lipidomics studies related to AFLD are needed.

Acknowledgment: We thank the Krystal J. Godri Pollitt Laboratory for computational resources.

REFERENCES

- 1) Ten Hove M, Pater L, Storm G, Weiskirchen S, Weiskirchen R, Lammers T, et al. The hepatic lipidome: from basic science to clinical translation. *Adv Drug Deliv Rev* 2020;159:180-197.
- 2) Reddy JK, Rao MS. Lipid metabolism and liver inflammation. II. Fatty liver disease and fatty acid oxidation. *Am J Physiol Gastrointest Liver Physiol* 2006;290:G852-G858.
- 3) World Health Organization. Global status report on alcohol and health 2018. <https://www.who.int/publications-detail-redirect/9789241565639>. Published September 27, 2018. Accessed May 2021.
- 4) Tsochatzis EA, Bosch J, Burroughs AK. Liver cirrhosis. *Lancet* 2014;383:1749-1761.
- 5) Grant BF, Chou SP, Saha TD, Pickering RP, Kerridge BT, Ruan WJ, et al. Prevalence of 12-month alcohol use, high-risk drinking, and DSM-IV alcohol use disorder in the United States, 2001-2002 to 2012-2013: results from the National Epidemiologic Survey on Alcohol and Related Conditions. *JAMA Psychiatry* 2017;74:911-923.
- 6) Arab JP, Roblero JP, Altamirano J, Bessone F, Chaves Araujo R, Higuera-De la Tijera F, et al. Alcohol-related liver disease: clinical practice guidelines by the Latin American Association for the Study of the Liver (ALEH). *Ann Hepatol* 2019;18:518-535.
- 7) Dugum M, McCullough A. Diagnosis and management of alcoholic liver disease. *J Clin Transl Hepatol* 2015;3:109-116.
- 8) Argemi J, Ventura-Cots M, Rachakonda V, Bataller R. Alcoholic-related liver disease: pathogenesis, management and future therapeutic developments. *Rev Esp Enferm Dig* 2020;112:869-878.
- 9) Bligh EG, Dyer WJ. A rapid method of total lipid extraction and purification. *Can J Biochem Physiol* 1959;37:911-917.
- 10) Koelmel JP, Kroeger NM, Gill EL, Ulmer CZ, Bowden JA, Patterson RE, et al. Expanding lipidome coverage using LC-MS/MS data-dependent acquisition with automated exclusion list generation. *J Am Soc Mass Spectrom* 2017;28:908-917.
- 11) Koelmel J, Sartain M, Salcedo J, Murali A, Li X & Stow S. Improving coverage of the plasma lipidome using iterative MS/MS data acquisition combined with lipid annotator software and 6546 LC/Q-TOF. Published June 30, 2020. <https://www.agilent.com/cs/library/applications/application-6546-q-tof-lipidome-5994-0775en-agilent.pdf>. Accessed May 2021.
- 12) Koelmel JP, Kroeger NM, Ulmer CZ, Bowden JA, Patterson RE, Cochran JA, et al. LipidMatch: an automated workflow for rule-based lipid identification using untargeted high-resolution tandem mass spectrometry data. *BMC Bioinformatics* 2017;18:331.
- 13) Koelmel JP, Cochran JA, Ulmer CZ, Levy AJ, Patterson RE, Olsen BC, et al. Software tool for internal standard based normalization of lipids, and effect of data-processing strategies on resulting values. *BMC Bioinformatics* 2019;20:217.
- 14) Koelmel JP, Aristizabal-Henao JJ, Ni Z, Fedorova M, Kato S, Otoki Y, et al. A novel technique for redox lipidomics using mass spectrometry: application on vegetable oils used to fry potatoes. *J Am Soc Mass Spectrom* 2021;32:1798-1809.
- 15) Ivanova PT, Milne SB, Myers DS, Brown HA. Lipidomics: a mass spectrometry based systems level analysis of cellular lipids. *Curr Opin Chem Biol* 2009;13:526-531.
- 16) Bowden JA, Heckert A, Ulmer CZ, Jones CM, Koelmel JP, Abdullah L, et al. Harmonizing lipidomics: NIST interlaboratory comparison exercise for lipidomics using SRM 1950-metabolites in frozen human plasma. *J Lipid Res* 2017;58:2275-2288.
- 17) Lanaspá MA, Andres-Hernando A, Orlicky DJ, Cicerchi C, Jang C, Li N, et al. Ketohehexokinase C blockade ameliorates fructose-induced metabolic dysfunction in fructose-sensitive mice. *J Clin Invest* 2018;128:2226-2238.
- 18) Clugston RD, Gao MA, Blaner WS. The hepatic lipidome: a gateway to understanding the pathogenesis of alcohol-induced fatty liver. *Curr Mol Pharmacol* 2017;10:195-206.
- 19) Wang Z, Yao T, Song Z. Involvement and mechanism of DGAT2 upregulation in the pathogenesis of alcoholic fatty liver disease. *J Lipid Res* 2010;51:3158-3165.
- 20) Zerbino DR, Achuthan P, Akanni W, Amode M, Barrell D, Bhai J, et al. Ensembl 2018. *Nucleic Acids Res* 2018;46:D754-D761.
- 21) Maceyka M, Spiegel S. Sphingolipid metabolites in inflammatory disease. *Nature* 2014;510:58-67.
- 22) Harizi H, Corcuff J-B, Gualde N. Arachidonic-acid-derived eicosanoids: roles in biology and immunopathology. *Trends Mol Med* 2008;14:461-469.
- 23) Clugston RD, Jiang H, Lee MX, Piantadosi R, Yuen JJ, Ramakrishnan R, et al. Altered hepatic lipid metabolism in C57BL/6 mice fed alcohol: a targeted lipidomic and gene expression study. *J Lipid Res* 2011;52:2021-2031.

- 24) Yang L, Jin G-H, Zhou J-Y. The role of ceramide in the pathogenesis of alcoholic liver disease. *Alcohol Alcohol* 2016;51:251-257. <https://doi.org/10.1093/alcalc/agg119>.
- 25) Liangpunsakul S, Sozio MS, Shin E, Zhao Z, Xu Y, Ross RA, et al. Inhibitory effect of ethanol on AMPK phosphorylation is mediated in part through elevated ceramide levels. *Am J Physiol Gastrointest Liver Physiol* 2010;298:G1004-G1012.
- 26) You M, Matsumoto M, Pacold CM, Cho WK, Crabb DW. The role of AMP-activated protein kinase in the action of ethanol in the liver. *Gastroenterology* 2004;127:1798-1808.
- 27) Van de Wiel A. The effect of alcohol on postprandial and fasting triglycerides. *Int J Vasc Med* 2012;2012:862504.
- 28) Bennett M, Gilroy DW. Lipid mediators in inflammation. *Microbiol Spectr* 2016;4.
- 29) González-Pérez A, Planagumà A, Gronert K, Miquel R, López-Parra M, Titos E, et al. Docosahexaenoic acid (DHA) blunts liver injury by conversion to protective lipid mediators: protectin D1 and 17S-hydroxy-DHA. *FASEB J* 2006;20:2537-2539.
- 30) Li Z, Agellon LB, Allen TM, Umeda M, Jewell L, Mason A, et al. The ratio of phosphatidylcholine to phosphatidylethanolamine influences membrane integrity and steatohepatitis. *Cell Metab* 2006;3:321-331.
- 31) Smith TL, Vickers A. Increases in liver microsomal phosphatidylethanolamine methyltransferase activity(s) in mice after short-term ethanol treatments. *Subst Alcohol Actions Misuse* 1984;5:131-140.
- 32) Morand OH, Zoeller RA, Raetz CR. Disappearance of plasmalogens from membranes of animal cells subjected to photosensitized oxidation. *J Biol Chem* 1988;263:11597-11606.
- 33) Skaff O, Pattison DI, Davies MJ. The vinyl ether linkages of plasmalogens are favored targets for myeloperoxidase-derived oxidants: a kinetic study. *Biochemistry* 2008;47:8237-8245.
- 34) Ikuta A, Sakurai T, Nishimukai M, Takahashi Y, Nagasaka A, Hui S-P, et al. Composition of plasmalogens in serum lipoproteins from patients with non-alcoholic steatohepatitis and their susceptibility to oxidation. *Clin Chim Acta* 2019;493:1-7.
- 35) Jang JE, Park H-S, Yoo HJ, Baek I-J, Yoon JE, Ko MS, et al. Protective role of endogenous plasmalogens against hepatic steatosis and steatohepatitis in mice. *Hepatology* 2017;66:416-431. Erratum in: *Hepatology* 2019;70:453.
- 36) Hauck AK, Bernlohr DA. Oxidative stress and lipotoxicity. *J Lipid Res* 2016;57:1976-1986.
- 37) Siler SQ, Neese RA, Hellerstein MK. De novo lipogenesis, lipid kinetics, and whole-body lipid balances in humans after acute alcohol consumption. *Am J Clin Nutr* 1999;70:928-936.
- 38) You M, Crabb DW. Molecular mechanisms of alcoholic fatty liver: role of sterol regulatory element-binding proteins. *Alcohol* 2004;34:39-43.
- 39) Rasineni K, Casey CA. Molecular mechanism of alcoholic fatty liver. *Indian J Pharmacol* 2012;44:299-303.
- 40) Régner M, Polizzi A, Guillou H, Loiseau N. Sphingolipid metabolism in non-alcoholic fatty liver diseases. *Biochimie* 2019;159:9-22.
- 41) Feldstein AE, Lopez R, Tamimi TAR, Yerian L, Chung Y-M, Berk M, et al. Mass spectrometric profiling of oxidized lipid products in human nonalcoholic fatty liver disease and nonalcoholic steatohepatitis. *J Lipid Res* 2010;51:3046-3054.

Author names in bold designate shared co-first authorship.

Supporting Information

Additional Supporting Information may be found at onlinelibrary.wiley.com/doi/10.1002/hep4.1825/supinfo.